



Published in final edited form as:

*Nucl Instrum Methods Phys Res A*. 2009 June 1; 604(1): 89–92. doi:10.1016/j.nima.2009.01.036.

## Low-Afterglow CsI:Tl microcolumnar films for small animal high-speed microCT

S.C. Thacker<sup>a</sup>, B. Singh<sup>a</sup>, V. Gaysinskiy<sup>a</sup>, E.E. Ovechkina<sup>a</sup>, S.R. Miller<sup>a</sup>, C. Brecher<sup>b</sup>, and V.V. Nagarkar<sup>a,\*</sup>

<sup>a</sup>RMD Inc., 44 Hunt Street, Watertown, MA 02472, USA

<sup>b</sup>ALEM Associates, 44 Hunt Street, Watertown, MA 02472, USA

### Abstract

Dedicated high-speed microCT systems are being developed for noninvasive screening of small animals. Such systems require scintillators with high spatial resolution, high light yield, and minimal persistence to ensure ghost free imaging. Unfortunately, the afterglow associated with conventional CsI:Tl microcolumnar films used in current high-speed systems introduces image lag, leading to substantial artifacts in reconstructed images, especially when the detector is operated at several hundreds of frames per second. At RMD, we have discovered that the addition of a second dopant, Eu<sup>2+</sup>, to CsI:Tl crystals suppresses the afterglow by as much as a factor of 40 at 2 ms after a short excitation pulse of 20 ns, and by as much as a factor of 15 at 2 ms after a long excitation pulse of 100 ms. Our observations, supported by theoretical modeling, indicate that Eu<sup>2+</sup> ions introduce deep electron traps that alter the decay kinetics of the material, making it suitable for many high-speed imaging applications. Here we report on the fabrication and characterization of CsI:Tl,Eu microcolumnar films to determine if the remarkable afterglow properties of CsI:Tl,Eu crystals are preserved in the CsI:Tl,Eu microcolumnar films. Preliminary results indicate that the codoped microcolumnar films show a factor of 3.5 improvement in the afterglow compared to the standard CsI:Tl films.

### Keywords

scintillators; cesium iodide; microcolumnar films; afterglow suppression; radiographic imaging

## 1. Introduction

CsI:Tl is one of the highly desired scintillator materials for medical and industrial applications. It has one of the highest conversion efficiencies of any known scintillator (62,000 photons/MeV), a rapid initial decay (680 ns), an emission in the visible range (540 nm), and a cubic structure that allows fabrication into microcolumnar films. It has a relatively high density (4.53 g/cm<sup>3</sup>), high atomic number (Z = 54), and is completely transparent to its own emitted light. In view of these excellent properties, along with its low cost and easy availability [1], CsI:Tl has been the material of choice for such applications as radiological imaging [2,3], x-ray and

\*Corresponding author. Tel.: +1-617-668-6937; fax: +1-617-926-9950; e-mail: vnagarkar@rmdinc.com.

**Publisher's Disclaimer:** This is a PDF file of an unedited manuscript that has been accepted for publication. As a service to our customers we are providing this early version of the manuscript. The manuscript will undergo copyediting, typesetting, and review of the resulting proof before it is published in its final citable form. Please note that during the production process errors may be discovered which could affect the content, and all legal disclaimers that apply to the journal pertain.

gamma ray spectroscopy, homeland security, and nuclear medicine applications such as intra-operative surgical probes and SPECT.

Despite the obvious advantages of CsI:Tl, however, it suffers from an intrinsic shortcoming that has hindered its use in CT and many other high-speed imaging applications: the presence of a persistent afterglow component in its scintillation decay. Although the initial decay has a characteristic time of 680 ns [2], its residual afterglow at 2 ms after the excitation can be as high as 5% of the peak value, depending on the intensity and duration of the excitation pulse. This causes pulse pileup in high count rate applications, reconstruction artifacts in CT applications, and problems of reduced contrast and image blurring in high speed x-ray imaging [2,3,4]. If the afterglow in CsI:Tl were significantly reduced, the material could be effectively used in many important modalities such as medical cone-beam or spiral CT, high speed small animal CT, fluoroscopic imaging, and time resolved X-ray diffraction imaging, enabling improved performance with substantial reduction in the cost.

During the past few years, we have been exploring the feasibility of suppressing this afterglow by chemical means. We have found that by codoping the CsI:Tl with  $\text{Eu}^{2+}$ , the afterglow in the time range of 10  $\mu\text{s}$ -100 ms can be lowered by almost two orders of magnitude. We have conducted an extensive investigation of this unusual effect [5], and have derived a detailed mathematical model that explains the underlying kinetic processes [6]. It is the purpose of this paper to discuss some of these results, outline recent developments in terms of fabricating CsI:Tl,Eu microcolumnar films for X-ray imaging applications, and to present their imaging characteristics. Implications of these developments with regard to actual imaging performance will also be described.

## 2. Materials

For the purposes of the current work, we measured the kinetic behavior of the scintillation from CsI:Tl,Eu in two distinct physical forms: single crystals and microcolumnar films. The crystals were grown by the familiar vertical Bridgman technique, where the raw material is melted in evacuated quartz ampoules, which are passed through a temperature gradient structured for optimal nucleation and growth of CsI single crystals. The resultant cylindrical boules (see Figure 1) were 10 mm in diameter and 35 mm long, from which disks were cut and polished to optical transparency, with a finished thickness of 2.5 mm. While the concentration of the  $\text{Eu}^{2+}$  codopant ranged between 0.05 and 0.5 mol percent, the bulk of the results we report here were obtained at 0.1 mol percent, nearly the same as that of the primary  $\text{Tl}^+$  activator.

Fabrication of the microcolumnar films is an entirely different matter. This represents a substantial challenge, since the films are deposited directly from the vapor phases of CsI, TlI, and  $\text{EuI}_2$ , and the vapor pressures of the three components differ by many orders of magnitude. Nevertheless, through systematic variation of the relevant parameters, we were able to define conditions for deposition of high-quality films ranging in thickness from 30  $\mu\text{m}$  to 1.3 mm onto graphite substrates. Representative SEMs are shown in Figure 2.

## 3. Decay Kinetics

For a number of years we have been conducting a comprehensive program [7] to characterize the mechanisms that govern the generation of afterglow in CsI:Tl and to suppress those mechanisms by means of selective incorporation of codopant ions. While most of the effects were modest [8], we have found that one particular ion,  $\text{Eu}^{2+}$ , exerts an afterglow-suppressive effect at least an order of magnitude greater than any of the others. The effect was most prominent under short-pulse (20 ns) excitation, as seen in Figure 3. Indeed, at 2 ms after the excitation pulse, the presence of  $\text{Eu}^{2+}$  reduces the afterglow by a factor as high as 40, depending on its concentration. In extensive studies of this phenomenon [9,10,11], we were able to fully

characterize the effect and were able to define the material composition that would provide optimal scintillation behavior. These studies [5] also found that the afterglow, expressed as a fraction of the intensity observed before excitation cut-off, was a strong function of the duration of the excitation pulse. Taking the same 2 ms elapsed time after excitation cut-off as a reference point, we have observed that the afterglow following a 100 ms excitation pulse is some two orders of magnitude higher than in the previous (short-pulse) case. Nevertheless, as Figure 3 shows, the suppressive effect is still substantial, a factor of more than 20.

We also performed such kinetic measurements on microcolumnar films, finding (Figure 4) that  $\text{Eu}^{2+}$  provides similar afterglow-suppressive effects here as well. This was by no means preordained, in view of the many fundamental differences between the two types of materials especially with regard to fabrication processing and crystallinity. Given that the vapor deposition is governed far more by kinetics than thermodynamics, it was by no means certain that the codopant would be incorporated into the CsI lattice at all, but just codeposited as an independent second phase. Thus we have laid this ghost to rest, finding an afterglow-suppressive effect in films that is quite comparable to that in single crystals. And while the magnitude of the effect (factors of 10 and 3.5 respectively for short- and long-pulse excitation) is not quite as great as in the crystal, this may merely reflect a shortfall in the  $\text{Eu}^{2+}$  content, which is not yet under adequate control. Even so, there is clearly enough to make substantial impact on the high-speed imaging performance, as we shall see shortly.

#### 4. Imaging Quality

To demonstrate the radiographic resolution capabilities of the new microcolumnar films, we used them to acquire images of a line-pair phantom used for evaluating mammographic imaging performance. The high spatial resolution and contrast are shown in Figure 5.

Even more striking are the images acquired from an actual biological phantom, a small fish measuring ~4 cm in length and ~1 cm in width. To achieve good contrast in imaging soft tissue and fine bones, we used 19 keV Mo X-rays from a GE Senograph mammography machine. These results are shown in Figure 6, where we can clearly see bone structure as thin as ~50  $\mu\text{m}$ , and can readily distinguish closely spaced bones in the background of soft tissue and the air sacs. Such performance is consistent with the measured spatial resolution of the film and is comparable to the best of the conventional (uncodoped) microcolumnar films.

#### 5. High-Speed Imaging

But the primary motivation for afterglow reduction is to enable more rapid acquisition of sequential radiographic images. Consequently, to demonstrate the extent to which the afterglow suppression can improve imaging performance under high-speed conditions, we integrated a 200  $\mu\text{m}$  thick CsI:Tl,Eu film into a special electron-multiplying CCD (EMCCD) camera available at RMD, and acquired X-ray images of a test phantom. For comparison we also evaluated a standard microcolumnar CsI:Tl screen produced by RMD, whose thickness was  $\approx 200 \mu\text{m}$ . The camera consisted of a back-thinned EMCCD containing a  $512 \times 512$  array of 16  $\mu\text{m}$  pixels, bonded to a 3:1 fiberoptic, giving an effective system resolution of  $\approx 50 \mu\text{m}$ . The camera has demonstrated very high sensitivity to 540 nm CsI:Tl emission and very low noise ( $< 1/e$ ) even when operated at high frame rates of 30 fps or above. Set for maximum contrast, this camera provides a dynamic imaging range well beyond that of commercial CCD systems, making it ideally suited for analyzing persistence in scintillator screens. The apparatus is illustrated in Figure 7.

For these tests the x-ray source was set to 300 kVp for a pulse of 20 ns. The EMCCD camera was used to acquire images 30 ms in duration, separated by a dead time of 1 ms. The test object, a tungsten coded aperture mask, was exposed to x-rays in a short pulse during the first

integration period only, with the subsequent frames acquiring their images with only the residual light provided by the afterglow. The resulting data for a conventional CsI:Tl screen and the new CsI:Tl,Eu film are shown in Figure 8.

As can be seen from these pictures, with conventional CsI:Tl a residual image is visible even after 8 frames (which is normally beyond the limited sensitivity of commercial CCD systems), whereas CsI:Tl codoped with  $\text{Eu}^{2+}$  shows virtually no residual image past the third frame. These data show that the afterglow suppression directly translates into dramatically improved dynamic radiography.

## 6. Conclusions

We have found the afterglow exhibited by CsI:Tl crystals to be substantially reduced by the addition of  $\text{Eu}^{2+}$  as a codopant. We have successfully vapor deposited microcolumnar films of CsI:Tl,Eu and have found that they also exhibit afterglow-suppressive effect. Films as thick as 1.3 mm have been fabricated, which show excellent columnar structure, high spatial resolution, and light emission efficiency similar to its undoped counterpart, CsI:Tl. In such films we have found that the frame-to-frame persistence of ghost images is reduced by an order of magnitude, paving the way for the use of CsI in fast imaging applications such as small animal high-speed microCT and radionuclide imaging. We are confident that further development will make the advantages of codoped CsI available for many other dynamic imaging applications from which it had previously been excluded.

## Acknowledgments

We thank the Public Health Service (NIH), DHHS for Grant No. 2R44CA001871-02A2, and the Medical Sciences Div., DOE, for Grant No. DE-FG02-04ER84054, which provided support for parts of this work.

## References

1. <http://www.bicron.com/>.
2. Rodnyi Piotr, A. Physical Processes in Inorganic Scintillators. CRC Press; Boca Raton, New York: 1997.
3. Knoll Glenn, F. Radiation Detection and Measurement. Second Edition. John Wiley & Sons; 1989.
4. Siewerdsen JH, Jaffray DA. A ghost story: Spatio-temporal response characteristics of an indirect-detection flat panel imager. *Med Phys* August;1999 26(8)
5. Brecher C, Lempicki A, Miller SR, Ovechkina EE, Gaysinskiy V, Nagarkar VV, Bartram RH. Suppression of afterglow in CsI:Tl by codoping with  $\text{Eu}^{2+}$  I. Experimental. *Nucl Instr & Meth A* 2006;558:450–457.
6. Bartram RH, Kappers LA, Hamilton DS, Lempicki A, Brecher C, Gaysinskiy V, Ovechkina EE. Suppression of afterglow in CsI:Tl by codoping with  $\text{Eu}^{2+}$  II. Theoretical model. *Nucl Instr & Meth A* 2006;558:458–467.
7. Reduced Afterglow CsI Scintillator for Medical Applications. Final Reports, SBIR Phase I and II Grants NIH9 R44 EB003382.
8. Brecher, C.; Nagarkar, VV.; Gaysinskiy, V.; Miller, SR.; Lempicki, A. Time-Resolved Studies of the Nonexponential Decay of CsI:Tl after Short-Pulse X-ray Excitation. *Nucl Inst & Meth*; presented at SCINT 2003; Valencia, Spain. Sept. 2003; 2005. p. 117-124.
9. Nagarkar VV, Ovechkina EE, Miller SR, Gaysinskiy V, Brecher C, Lempicki A, Bartram RH. Luminescence properties of CsI:Tl crystals codoped with Eu. *Functional Materials* 2005;12:645–652.
10. Brecher, C.; Ovechkina, EE.; Gaysinskiy, V.; Miller, SR.; Nagarkar, VV.; Bartram, RH.; Lempicki, A. Afterglow suppression in codoped CsI:Tl,Eu and its effect on imaging speed. *Proc 8th Intl Conf Inorg Scint., SCINT2005*; Alushta, Ukraine. Sept. 2005; p. 407-410.
11. Ovechkina, EE.; Gaysinskiy, V.; Miller, SR.; Brecher, C.; Lempicki, A.; Nagarkar, VV. Multiple doping of CsI:Tl crystals and its effect on afterglow. presented at 6th European Conference on

Luminescent Detectors and Transformers of Ionizing Radiation, LUMDETR2006; Lviv, Ukraine.  
June 2006;



**Fig. 1.** A photograph of typical CsI:Tl and CsI:Tl,Eu single crystal boules grown at RMD, illuminated by their own UV-excited fluorescence. Note enhanced blue color, from emission added by Eu<sup>2+</sup>.

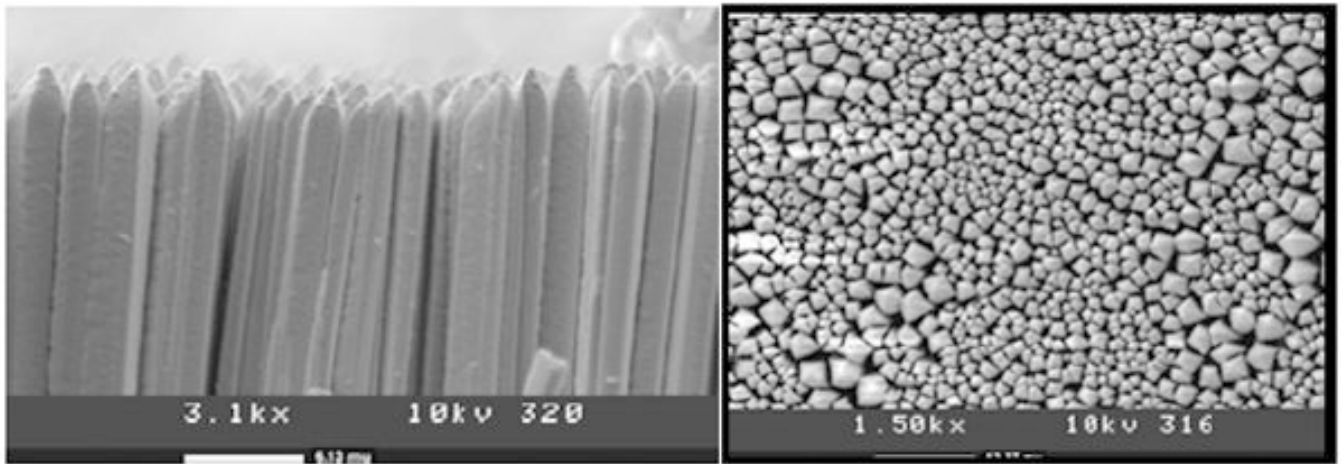


**Fig. 2.**  
SEMs of a 200  $\mu\text{m}$  thick microcolumnar CsI:Tl,Eu film developed at RMD. Left, well-separated columns of the film; right, the corresponding top view

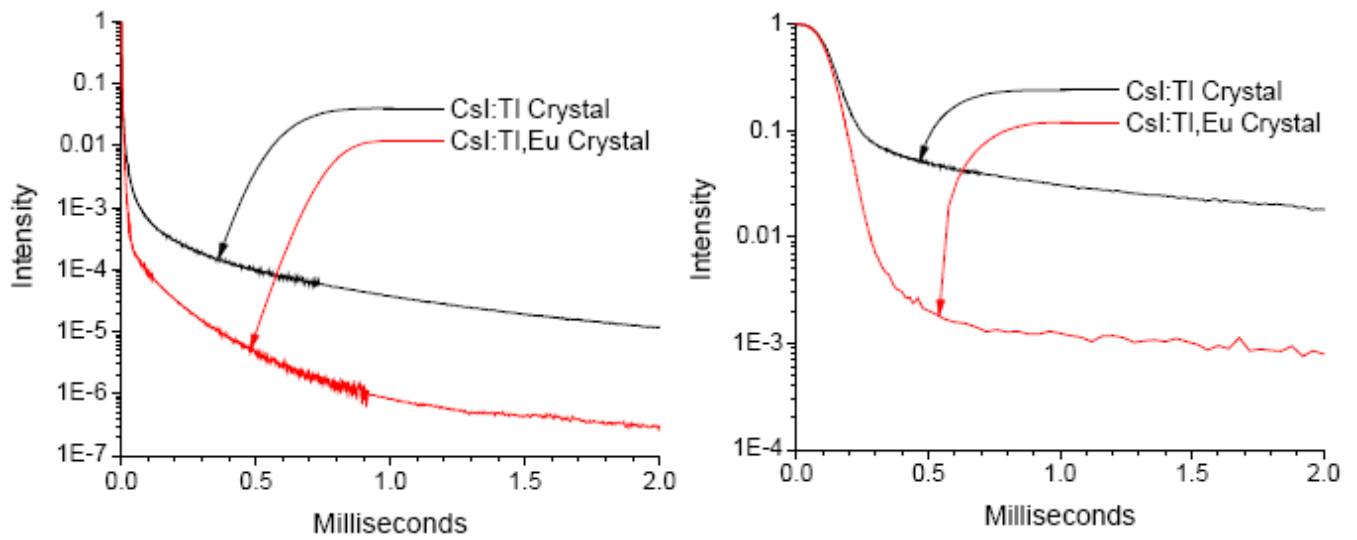


**Fig. 3.** Semilog plots of the scintillation decay of CsI:Tl crystals with and without the decay-modifying additive  $\text{Eu}^{2+}$ . Left, after short-pulse (20 ns) and right, after long-pulse (100 ms) excitation. Note that while the long pulse generates a higher level of afterglow, the  $\text{Eu}^{2+}$  additive provides a comparable suppressive effect under both excitation conditions.



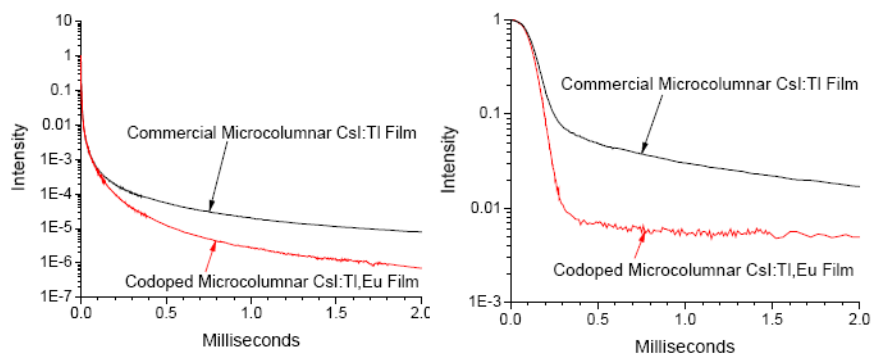


**Fig. 4.** Semilog plots of the scintillation decay of microcolumnar CsI:Tl films with and without the decay-modifying additive  $\text{Eu}^{2+}$ . Left, after short-pulse (20 ns) and right, after long-pulse (100 ms) excitation. Although here the afterglow-suppressive effect provided by the  $\text{Eu}^{2+}$  additive is somewhat less than in single crystals, this may merely indicate a lower concentration.

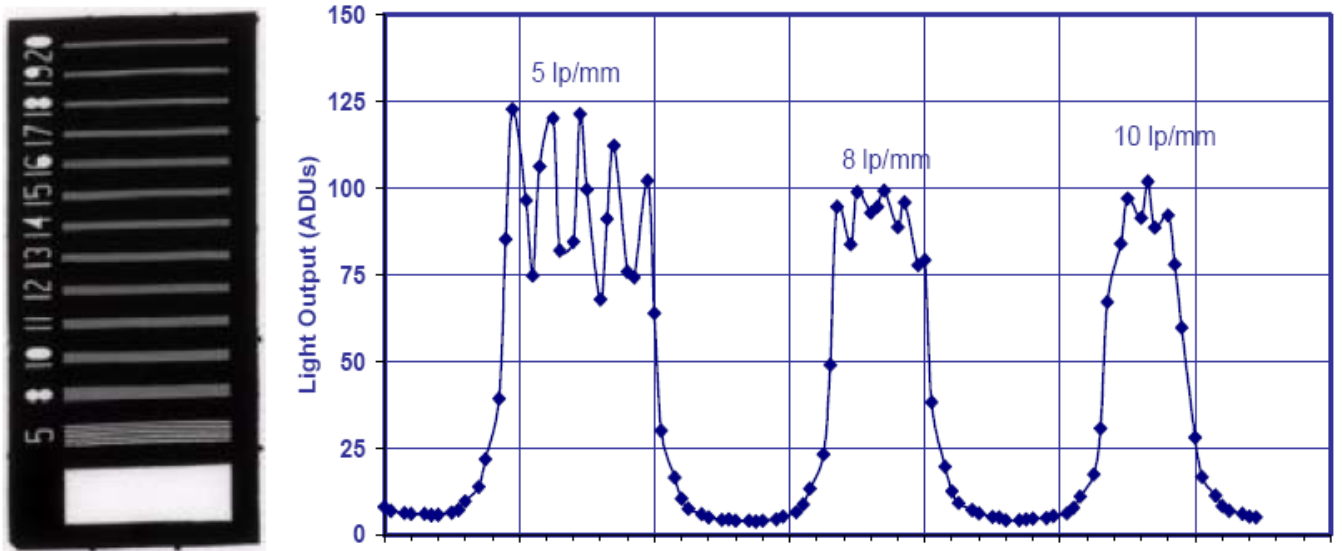


**Fig. 5.** Radiographic imaging of a mammography line pair phantom using a 200  $\mu\text{m}$  microcolumnar CsI:Tl,Eu film coupled to a CCD with Nyquist limiting resolution of 11 lp/mm. Left is an acquired image of the phantom; right shows an intensity trace along its length.



**Fig. 6.** Radiograph of a small fish taken using a 200- $\mu\text{m}$  thick microcolumnar CsI:Tl, Eu film. Note well-resolved fine bone structure ( $<100\ \mu\text{m}$ ) and excellent contrast between the background tissue and the air sacs.

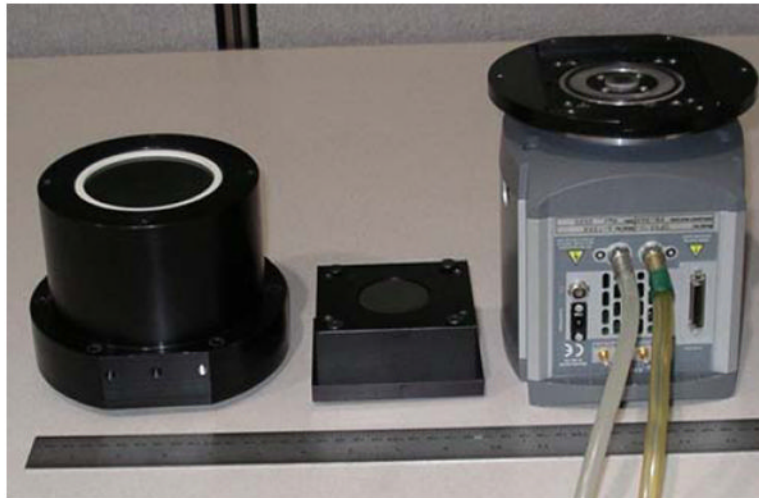


**Fig. 7.**  
EMCCD camera used for dynamic imaging: Detector is  $512 \times 512$  array of  $16 \mu\text{m} \times 16 \mu\text{m}$  pixels.  
Camera was operated at 30 fps

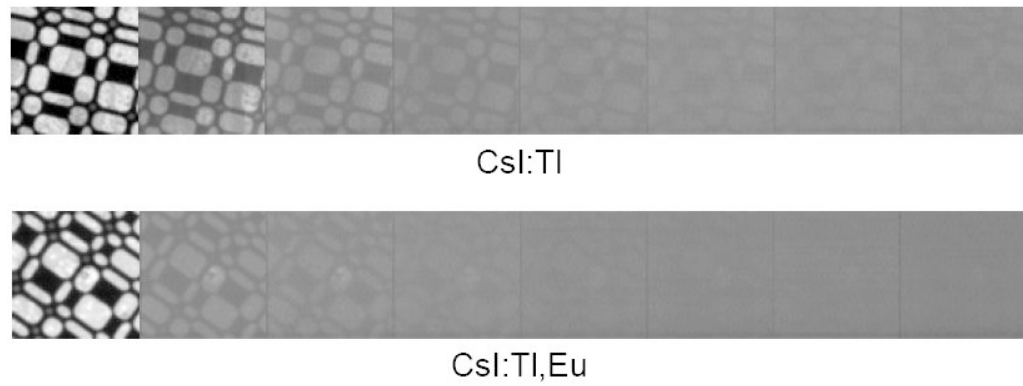


**Fig. 8.**

Dynamic imaging of a tungsten coded aperture mask after 20 ns excitation using microcolumnar CsI:Tl films without and with  $\text{Eu}^{2+}$  to suppress afterglow. Each frame lasts 30 ms and is separated from the next by 1 ms. The X-ray pulse occurs during the first frame only, but the image in CsI:Tl persists even after 8 frames. The corresponding data for CsI:Tl,Eu shows virtually no residual image after 3 frames, demonstrating the practical utility of this new material.